HIGH-FREQUENCY BACKSCATTERING FROM A FINITE CONE

T.B.A. Senior[+] and P.L.E. Uslenghi[++]

Abstract

The high-frequency backscattered field produced by a plane electromagnetic wave at oblique incidence on a perfectly conducting, right circular cone with a flat base is considered. The first two terms of the asymptotic expansion are obtained by applying the geometrical theory of diffraction and these reduce to previously-derived results in the particular case of a circular disk.

Due to the axial caustic, functions must be introduced to match the wide-angle formulae to the known results for nose-on incidence. This matching is effected by employing Bessel functions and Fresnel integrals for the first and second-order terms, respectively. The resulting expressions are valid for all cone angles and for a wide range of aspect angles about nose-on, and are found to be in good agreement with experimental data.

1. Introduction

Over the last dozen years the problem of the backscattering of electromagnetic waves by a flat-based or right circular cone of finite length has excited a great deal of interest. On the practical side, this shape is often used as a prototype for missiles and re-entry vehicles and this fact has stimulated a number of theoretical investigations of the scattering. On the theoretical side, the shape is of sufficient complexity to pose a problem that is challenging, yet simple enough to hold out the lure of accurate estimates of the scattering.

[+] Radiation Laboratory, The University of Michigan, Ann Arbor, Michigan 48108

[++] Department of Information Engineering, University of Illinois at Chicago Circle, Chicago, Illinois 60680

We shall consider here the case of a perfectly conducting cone of half angle γ, and seek an expression for the backscattered field for large ka, where a is the base radius. The first effective estimate of the base contribution to the scattering was provided by Siegel (1958) using circular wedge theory in which each portion of the rim is assumed to scatter as would an element of the corresponding wedge. Siegel considered only axial incidence, but shortly afterwards Keller (1960) applied his geometrical theory of diffraction to the cone and produced first order estimates of the backscattered field for all incidence angles bounded away from the caustic directions. No attempt was made to provide caustic matching functions to smooth the transitions from one angular range to another, but in the particular case of incidence along the axis (which is itself a caustic), Keller carried through his theory to the second order by including the contribution of waves which have traversed the rear of the cone once. A rather limited comparison of theoretical and measured data for the axial cross section has been given by Keller (1961).

A more extensive comparison of theory with experiment has been provided by Bechtel (1965), who also corrects errors in Keller's original expressions. Using Keller's first order expressions with no attempt at caustic matching, Bechtel observes that for angles near to nose-on incidence the agreement with experiment is quite good for horizontal polarization but very poor for vertical polarization.

In order to remove this discrepancy, it is essential to provide some form of matching of the 'wide angle' expressions into the axial caustic. This problem has been explored by Ross (1969) who has produced a matching of the first order expressions for both vertical and horizontal polarizations that incorporates Bessel functions of the first three orders and is similar to that given by Ufimtsev (1958) for a disk. Ryan and Peters (1969, but see 1970) have also tried to produce

results that would be valid in the vicinity of the axial caustic, using postulated distributions for the surface field components near to the rim of the base. However, the expressions that they obtain appear theoretically improbable, and are not supported by experimental data.

The present paper is also concerned with the high frequency backscattering from a cone at angles from axial incidence ($\Phi = 0$) out to, and just beyond, the backward cone angle, $\Phi = \gamma$. For Φ bounded away from zero, the geometrical theory of diffraction is used to obtain the first and second order terms in the scattered field. The latter are here obtained for the first time, and in the case of E polarization, are of particular interest because of the unusual ray paths across the base of the cone that permit this second order contribution to be observed even for $\Phi > \gamma$. It is shown that the matching of both the first and second order terms into the axial caustic is directly analogous to the problem previously considered (Knott et al, 1970) for a disk. Indeed, the same matching functions occur, leading to a 'uniform' asymptotic expansion for $0 \leq \Phi < \gamma$. The agreement with experiment is superior to any previously obtained.

2. The Second-Order Backscattered Field

The scattering body is a perfectly conducting right circular cone with semi-aperture angle γ and base radius a, immersed in free space. The geometry is illustrated in Figure 1, where the cone is viewed both along its axis, z, of symmetry and in a direction perpendicular to it (i.e. along the x-axis). An incident plane electromagnetic wave with wave number k propagates in the direction of the unit vector $\hat{i}$ parallel to the (y, z) plane and forming the angle Φ with the negative z-axis and the angle $(\pi/2 - \Phi)$ with the negative y-axis:

$$\hat{i} = -\hat{y} \sin \Phi - \hat{z} \cos \Phi . \qquad (1)$$

We consider the two cases of E-polarization, in which the incident electric field is

$$\underline{E}^i = \hat{x} \exp\{- ik (y \sin \Phi + z \cos \Phi)\}, \tag{2}$$

and H-polarization, in which the incident magnetic field is

$$\underline{H}^i = \hat{x} \exp\{- ik (y \sin \Phi + z \cos \Phi)\} ; \tag{3}$$

the time-dependence factor $\exp(-i\omega t)$ is omitted throughout. In the former case the far backscattered electric field may be written as

$$\underline{E}^{b.s.} = \hat{x} \frac{e^{ikr}}{kr} S_E , \tag{4}$$

whereas in the latter the far backscattered magnetic field is

$$\underline{H}^{b.s.} = \hat{x} \frac{e^{ikr}}{kr} S_H , \tag{5}$$

where r is the distance of the observation point from the center O of the cone base. In terms of the quantity S, the backscattering cross section is

$$\sigma = \frac{\lambda^2}{\pi} |S|^2 , \tag{6}$$

where $\lambda = 2\pi/k$ is the wavelength. When the characteristic dimensions of the scatterer are large compared with the wavelength ($ka >> 1$), the far-field coefficients S_E and S_H can be expanded asymptotically in series of inverse (fractional) powers of ka. In the following, the first two terms of these series are derived.

To obtain the backscattered field via the geometrical theory of diffraction (see, for example, Keller 1957, 1962; Keller and Hansen, 1965), we must determine the paths of all reflected and diffracted rays which pass through the

observation point, the divergence factors along these rays, and the diffraction coefficients at each point of diffraction. The field along a ray diffracted at a tip or at an edge is therefore the product of four factors: the diffraction coefficient, the incident field at the point of diffraction, the divergence factor, and a phase delay proportional to the distance from the point of diffraction. The ray paths are discussed in section 2.1, the divergence factors and diffraction coefficients are determined in sections 2.2 and 2.3, and the second-order backscattered field is obtained in section 2.4.

2.1 Ray Tracing

The first-order terms in the asymptotic expansions of S_E and S_H are produced by singly diffracted rays backscattered from the circular edge at the base of the cone. For $\Phi = 0$, all points of the edge contribute, whereas for oblique incidence within the backward cone (i.e. for $0 < \Phi < \gamma$) there are only two first-order rays, and these are backscattered from the flash points P_1 and P_2 at which the edge intersects the plane (y, z) of incidence (Figure 1). For $\gamma < \Phi < \pi/2$, the flash point P_2 is not illuminated by the primary wave, so that only the ray backscattered from P_1 is to be taken into account.

The determination of the second-order terms in the expansions of S_E and S_H is more complicated. For $\Phi = 0$, these terms originate from the cylindrical surface of backscattered rays which have been doubly diffracted at any two opposite points of the circular rim of the cone.

For $\Phi \neq 0$, the contributions to the second-order terms come from the ray singly diffracted at the tip and from the rays doubly diffracted at the base of the cone. The latter can be determined by recalling that, according to the geometrical theory, the incident and diffracted rays lie on opposite sides of the plane normal to the edge, and the diffracted rays are the generators of a cone

whose axis is tangent to the edge at the diffraction point and whose half angle is the angle between the incident ray and the tangent. If these rules are applied to two successive edge diffractions of the same ray, four doubly diffracted rays are found. Two such rays are those incident at P_1 (or P_2), diffracted toward P_2 (or P_1) and backscattered from P_2 (or P_1). The other two are 'migrating' rays which strike the edge at points P_3 and P_4 symmetrically located with respect to the (y, z) plane (see Figure 1), and which were noted for the first time by Knott et al (1970) in connection with a disk. The distance of P_3 and P_4 from the x-axis is

$$a \sin \Phi \Big/ \sqrt{1 + \sin^2 \Phi} \quad ,$$

and the azimuth ϕ of P_3 (taken as positive) is

$$\phi = \arccos \frac{1}{\sqrt{1 + \sin^2 \Phi}} \quad , \tag{7}$$

implying that $0 < \phi < \pi/4$.

The rays doubly diffracted at P_1 and P_2 occur only within the backward cone (i.e. for $\Phi < \gamma$), but the migrating rays doubly diffracted at P_3 and P_4 occur for all $\Phi \leq \Phi_{max}$, where $\Phi_{max} > \gamma$. At $\Phi = \Phi_{max}$, the points P_3 and P_4 are on the shadow boundary, and for $\Phi > \Phi_{max}$ they lie within the shadow region. The value of Φ_{max} is found by observing that the outward unit normal to the conical surface is

$$\hat{n} = \hat{x} \cos\gamma \cos\psi - \hat{y} \cos\gamma \sin\psi + \hat{z} \sin\gamma \, , \tag{8}$$

and that the equation of the shadow boundary is $\hat{i} \cdot \hat{n} = 0$, with $\hat{i}$ given by (1). The shadow boundary is therefore a generator whose azimuth ψ (taken as positive)

is

$$\psi = \arcsin(\tan\gamma \cot\Phi) \ , \tag{9}$$

and if P_3 and P_4 are to lie within the illuminated region, i.e. $\phi \leq \psi$, it follows from (7) and (9) that

$$\Phi_{max} = \arcsin\sqrt{\sin\gamma} \ . \tag{10}$$

A plot of Φ_{max} as a function of γ is shown in Figure 2. Observe that Φ_{max} exceeds the angle $(\pi/2 - \gamma)$ of the specular flash if $\gamma > 38.2$ degrees.

2.2 Divergence Factors

The divergence factor $\Gamma_{hj\ell}$ at a point P_ℓ along a ray diffracted at the edge point P_j, and corresponding to an incident ray coming from P_h, is (see, for example, Keller 1962);

$$\Gamma_{hj\ell} = \sqrt{\frac{\rho_{hj\ell}}{(\rho_{hj\ell} + s_{j\ell})\, s_{j\ell}}} \ , \tag{11}$$

where $s_{j\ell}$ is the distance between P_j and P_ℓ, while $\rho_{hj\ell}$ is the distance from the edge point P_j to the caustic of the diffracted rays, measured negatively in the direction of propagation. The radius of curvature, ρ, of the diffracted wavefront may be written in the two equivalent forms:

$$\rho = \frac{-a \sin^2\beta}{a \sin\beta \frac{\partial\beta}{\partial\tau} + \cos\delta} = \frac{a \sin^2\beta}{(\hat{u} - \hat{d}) \cdot \hat{n} + a\hat{\tau} \cdot \frac{\partial\hat{u}}{\partial\tau}} \ , \tag{12}$$

where τ is the arclength along the edge, β is the angle between the incident unit vector $\hat{u}$ and the tangent unit vector $\hat{\tau}$, and δ is the angle between the

principal normal to the edge (i.e. the normal pointing toward the center of curvature) and a unit vector $\hat{d}$ oriented in the direction of the diffracted ray. The quantity ρ remains unchanged when the direction of increasing arclength τ is reversed. Observe that in the second of the above expressions for ρ, the term $\partial u/\partial\tau$ is zero only when the field incident on the edge is a locally plane wave.

It is found that for the singly diffracted rays

$$\rho_{i\,1\,r} = -\rho_{i\,2\,r} = \frac{a}{2\sin\Phi}\,, \tag{13}$$

whereas for the doubly diffracted rays

$$\rho_{i\,1\,2} = \frac{-a}{1-\sin\Phi}\,, \qquad \rho_{1\,2\,r} = a\,\frac{1-2\sin\Phi}{2\sin^2\Phi}\,,$$

$$\rho_{i\,2\,1} = \frac{-a}{1+\sin\Phi}\,, \qquad \rho_{2\,1\,r} = a\,\frac{1+2\sin\Phi}{2\sin^2\Phi}\,,$$

$$\rho_{i\,3\,4} = \rho_{i\,4\,3} = -a\,(1+\sin^2\Phi)^{-3/2} \tag{14}$$

$$\rho_{3\,4\,r} = \rho_{4\,3\,r} = -a\,\frac{1+2\sin^2\Phi}{2\sin^2\Phi}\,(1+\sin^2\Phi)^{-3/2}$$

in which the subscripts "i" and "r" indicate the incident and backscattered directions, respectively. Since there is a phase delay of $\pi/2$ in crossing a caustic line, our time convention requires us to take $\sqrt{-1} = -i$ whenever $\Gamma^2 > 0$.

2.3 Diffraction Coefficients

For the diffraction coefficients D we adopt the same notation involving three subscripts used for the divergence factors. If the incident wave is either E or H polarized, D can be considered a scalar for the rays diffracted at P_1

and P_2; by using the wedge diffraction coefficients of Keller (1960; footnote 15), we obtain:

$$D_{i1r} = A_o \left[(\cos\frac{\pi}{n} - 1)^{-1} \mp \left(\cos\frac{\pi}{n} - \cos\frac{2(\gamma + \Phi)}{n} \right)^{-1} \right], \quad (15)$$

$$D_{i2r} = A_o \left[(\cos\frac{\pi}{n} - 1)^{-1} \mp \left(\cos\frac{\pi}{n} - \cos\frac{2(\gamma - \Phi)}{n} \right)^{-1} \right], \quad (16)$$

$$D_{i12} = A_o \left[\left(\cos\frac{\pi}{n} - \cos\frac{3\pi - 2\Phi}{2n} \right)^{-1} \mp \left(\cos\frac{\pi}{n} - \cos\frac{3\pi - 2\Phi}{2n} \right)^{-1} \right], \quad (17)$$

$$D_{i21} = A_o \left[\left(\cos\frac{\pi}{n} - \cos\frac{3\pi + 2\Phi}{2n} \right)^{-1} \mp \left(\cos\frac{\pi}{n} - \cos\frac{3\pi + 2\Phi}{2n} \right)^{-1} \right], \quad (18)$$

$$D_{21r} = A_o \left[\left(\cos\frac{\pi}{n} - \cos\frac{3\pi - 2\Phi}{2n} \right)^{-1} \mp \left(\cos\frac{\pi}{n} - \cos\frac{3\pi - 2\Phi}{2n} \right)^{-1} \right], \quad (19)$$

$$D_{12r} = A_o \left[\left(\cos\frac{\pi}{n} - \cos\frac{3\pi + 2\Phi}{2n} \right)^{-1} \mp \left(\cos\frac{\pi}{n} - \cos\frac{3\pi + 2\Phi}{2n} \right)^{-1} \right], \quad (20)$$

where

$$A_o = \frac{e^{i\frac{\pi}{4}} \sin\frac{\pi}{n}}{n\sqrt{2\pi k}}, \quad (21)$$

$$n = \frac{3}{2} + \frac{\gamma}{\pi}, \quad (22)$$

and the upper (lower) sign refers to E (H) polarization.

Observe that the diffraction coefficients of formulas (17) - (20) are zero for E polarization. Thus, the rays through the flash points P_1 and P_2 contribute to the second-order term in the expansion of S_H only, and the contribution of the edge-diffracted rays to the second-order term in S_E arises solely from the rays doubly diffracted at the migrating points P_3 and P_4. In reality, the diffraction coefficients are asymptotic expansions in inverse fractional powers of k of which we here consider only the leading term (see, for example, Buchal and Keller, 1960). Although the complete diffraction coefficients are not exactly zero for E polarization, they only contribute to terms higher than the second in the expansions of the far-field coefficients.

For the rays obliquely incident at P_3 and P_4, the diffraction coefficient is a 3 x 3 matrix which, in the limiting case of a screen of zero thickness ($\gamma = \pi/2$), has been given explicitly by Keller (1957). Keller's matrix is easily generalized to a wedge of arbitrary angle; however, it is not unique and, in its original form, it is not suited to the case in which the incident or diffracted rays graze one of the faces of the wedge. This defect can be remedied, and since the resulting matrix should prove useful in a variety of problems, its derivation is presented in the Appendix. The fundamental result is given in Eq. (A-13), and the matrix elements are specified in Eqs. (A-9). The diffraction matrix multiplies the incident electric field at the point of diffraction, expressed as a column vector in terms of its components along the axes of a local, right-handed Cartesian coordinate system whose unit vectors $\hat{T}$, $\hat{N}$, $\hat{B}$ are described in the Appendix.

2.4 Backscattered Field

For a large cone base ($ka >> 1$) and oblique incidence ($\Phi \neq 0$), the far-field coefficients may be expanded in the form

$$S_{E,H} \sim S^{I}_{E,H} + S^{II}_{E,H} + O\left[(ka)^{-1/2}\right], \tag{23}$$

where the first-order terms $S^{I}_{E,H}$ are proportional to $\sqrt{ka}$ and the second-order terms $S^{II}_{E,H}$ are of order unity.

The first-order terms are

$$\frac{e^{ikr}}{kr} S^{I} = D_{i1r} \Gamma_{i1r} e^{ik(\psi_1 + s_{1r})} + D_{i2r} \Gamma_{i2r} e^{ik(\psi_2 + s_{2r})}, \tag{24}$$

where $k\psi_1$ and $k\psi_2$ are the phases of the incident field at P_1 and P_2, respectively. Hence,

$$\left.\begin{matrix}\psi_1 \\ \psi_2\end{matrix}\right\} = \mp a \sin\Phi \quad , \quad \left.\begin{matrix}s_{1r} \\ s_{2r}\end{matrix}\right\} = r \mp a \sin\Phi \ . \tag{25}$$

By using the results of sections 2.2 and 2.3, it is found that

$$S^{I}_{\substack{E \\ H}} = \frac{\sin\frac{\pi}{n}}{2n}\sqrt{\frac{ka}{\pi \sin\Phi}}\left\{\left[\left(\cos\frac{\pi}{n} - 1\right)^{-1} \mp \left(\cos\frac{\pi}{n} - \cos\frac{2(\gamma-\psi)}{n}\right)^{-1}\right] e^{2ika\sin\Phi - i\frac{\pi}{4}} + \right.$$

$$\left. + \left[\left(\cos\frac{\pi}{n} - 1\right)^{-1} \mp \left(\cos\frac{\pi}{n} - \cos\frac{2(\gamma+\psi)}{n}\right)^{-1}\right] e^{-2ika\sin\Phi + i\frac{\pi}{4}}\right\}, \tag{26}$$

which is valid under the condition

$$r >> \frac{a}{2\sin\Phi}, \tag{27}$$

i.e. Φ bounded away from zero as r tends to infinity. Result (27) agrees with that of Bechtel (1965).

The contributions to the second-order terms arise from the ray singly diffracted at the tip and from the four rays doubly diffracted at the base of the cone. When the calculations are performed for the doubly diffracted rays, it is found that the two rays diffracted at P_1 and P_2 contribute only for H polarization, whereas the two rays diffracted at P_3 and P_4 contribute only for E polarization. In the former case

$$\frac{e^{ikr}}{kr} S_H^{II} = D_{i12} D_{12r} \Gamma_{i12} \Gamma_{12r} e^{ik(\psi_1 + 2a + s_{2r})} +$$

$$+ D_{i21} D_{21r} \Gamma_{i21} \Gamma_{21r} e^{ik(\psi_2 + 2a + s_{1r})} \quad . \tag{28}$$

By using the results of sections 2.2 and 2.3, and invoking the condition that

$$r >> a \frac{1 + 2 \sin \Phi}{2 \sin^2 \Phi} \quad , \tag{29}$$

equation (28) becomes

$$S_H^{II} = \frac{2e^{2ika}}{\pi \sin \Phi} G(\Phi) \quad , \tag{30}$$

where

$$G(\Phi) = \frac{\left(\frac{1}{n} \sin \frac{\pi}{n}\right)^2}{\left(\cos \frac{\pi}{n} - \cos \frac{3\pi - 2\Phi}{2n}\right)\left(\cos \frac{\pi}{n} - \cos \frac{3\pi + 2\Phi}{2n}\right)} \quad . \tag{31}$$

In particular, for a disk ($\gamma = \pi/2$, $n = 2$), equation (30) reduces to

$$S_H^{II}\Big|_{disk} = \frac{e^{2ika}}{\pi \sin\bar{\Phi}\cos\bar{\Phi}} , \tag{32}$$

in agreement with the result obtained by Knott et al (1970).

In the case of E polarization

$$\frac{e^{ikr}}{kr} S_E^{II} = \Gamma_{i34}\Gamma_{34r} e^{ik(\psi_3+2a\cos\psi+s_{4r})} D_{34r}\left\{D_{i34}\underline{E}_3^i\right\}$$

$$+\Gamma_{i43}\Gamma_{43r} e^{ik(\psi_4+2a\cos\psi+s_{3r})} D_{43r}\left\{D_{i43}\underline{E}_4^i\right\} , \tag{33}$$

where

$$\psi_3 = \psi_4 = \frac{a\sin^2\bar{\Phi}}{\sqrt{1+\sin^2\bar{\Phi}}} , \tag{34}$$

$$s_{3r} = s_{4r} = r + \psi_3 , \tag{35}$$

and $\bar{\phi}$ is given by (7). The incident fields $\underline{E}_3^i$ and $\underline{E}_4^i$ are the field of eq. (2), expressed as column vectors in terms of the local bases $\hat{T}$, $\hat{N}$, $\hat{B}$ at the points P_3 and P_4, respectively. The column vectors $\left\{D_{i34}\underline{E}_3^i\right\}$ and $\left\{D_{i43}\underline{E}_4^i\right\}$ must also be expressed in terms of the local bases at P_4 and P_3. When the results of sections 2.2 and 2.3 and of the Appendix are taken into account, and the appropriate coordinate transformations are performed, it is found that with the condition

$$r >> \left|\rho_{34r}\right| , \tag{36}$$

equation (33) becomes

$$S_E^{II} = \frac{2i\cos^2\Phi\sqrt{1+\sin^2\Phi}}{\pi\sin\Phi} E(\Phi)\, e^{2ika\sqrt{1+\sin^2\Phi}}, \tag{37}$$

where

$$E(\Phi) = \left\{ \frac{\frac{1}{n}\sin\frac{\pi}{n}}{\cos\frac{\pi}{n} - \cos\frac{3\pi + 2\alpha_o}{2n}} \right\}^2, \tag{38}$$

with

$$\alpha_o = \arcsin(\sin^2\Phi) . \tag{39}$$

In particular, for a disk ($\gamma = \frac{\pi}{2}$, $n = 2$),

$$E(\Phi)\Big|_{disk} = \frac{1}{2(1+\sin^2\Phi)} \tag{40}$$

and equation (37) therefore yields

$$S_E^{II}\Big|_{disk} = \frac{i\cos^2\Phi}{\pi\sin\Phi\sqrt{1+\sin^2\Phi}}\, e^{2ika\sqrt{1+\sin^2\Phi}}, \tag{41}$$

which is a previously-derived result (Knott et al, 1970).

As noted earlier, the tip also provides a contribution to the scattered field that is the same order in k as the contribution of the doubly diffracted edge rays at oblique incidence. Using the known solution for the scattering of a plane wave by a semi-infinite cone, expressions for the tip contribution, S^{tip}, can be derived for either large or small γ. In particular, Felsen (1957) has shown that

$$S_E^{tip} \approx -i\, \frac{\sin^2(\frac{1}{2}\gamma)}{\cos^3\Phi} (1 - \tfrac{1}{4}\sin^2\Phi)\, e^{2ika\cot\gamma\cos\Phi}, \tag{42}$$

valid for $\gamma << 1$ and $0 \leq \Phi < \frac{\pi}{2} - \gamma$, where the phase factor has been included to transfer the phase origin to the center of the base. Higher order terms in γ have been given by Bowman et al (1969, pp. 675 et seq), who also show that

$$S_H^{tip} \approx i\left\{\frac{\tan^2\frac{1}{2}\Phi}{2\ell n(\sin^2\frac{1}{2}\gamma)\cos\Phi} + \frac{\sin^2\frac{1}{2}\gamma}{\cos^2\Phi}(1 - \frac{1}{2}\sin^2\Phi)\right\} e^{2ika\cot\gamma\cos\Phi}, \tag{43}$$

valid under the same conditions. Both expressions are increasing functions of Φ and are consistent with the physical optics result (which is independent of polarization) only for $\Phi = 0$.

Although mathematical completeness would require the inclusion of the above tip contributions in any second-order treatment of cone scattering, the magnitude of $\left|S_{E,H}^{tip}\right|$ is such that it is negligible compared with the base contributions that are present. For example, with $\gamma = 15^o$, $\left|S_{E,H}^{tip}\right|$ is less than -35dB for $\Phi = 0$, increasing by less than 5dB as Φ increases to 30^o. We shall therefore ignore this contribution throughout the subsequent discussion.

The resulting second-order approximation to the high-frequency backscattered field for oblique incidence is represented by formulae (23), (26), (30) and (37). While the first-order expressions (26) are well known, the second-order results (30) and (37) are given here for the first time.

3. Matching Into the Axial Caustic

For axial incidence the geometrical theory of diffraction gives (Keller, 1960)

$$S_{E,H}^{I} = \mp ka\, B_o , \tag{44}$$

$$S^{\Pi}_{E,H} = \mp \sqrt{\frac{ka}{\pi}}\, e^{2ika - i\pi/4}\, E(0) \ , \tag{45}$$

where

$$B_o = \frac{1}{2n \sin \frac{2\pi}{n}} \tag{46}$$

and E(0) is given by (38) with $\Phi = 0$. Because of the axial caustic, these results cannot be obtained merely by putting $\Phi = 0$ in Eqs. (26), (30) and (37), and we must now introduce caustic matching functions which will serve to interpolate between the wide-angle and on-axis formulae.

In a purely mathematical sense, such 'smoothing' is only important in the immediate vicinity of $\Phi = 0$, i.e., in an angular range which tends to zero as $ka \rightarrow \infty$. In practice, however, we often require to compute the scattering when ka is as small as 10 (or less). The expressions for the scattered field incorporating the matching functions may then differ from the wide angle formulae throughout the entire backward cone ($\Phi \leq \gamma$) and beyond, and the choice of matching function is no longer an academic matter.

Although the geometric theory does not provide a unique specification of the matching functions, the matching problem is identical to that which arises in scattering from a disk. In their study of disk scattering, Knott et al (1970) obtained a match which was supported conceptually and experimentally, and the requirement that the caustically-corrected cone solution degenerate to the disk solution when $\gamma = \pi/2$ can be used to specify the matching functions in the present case.

Let us start by considering the first order terms. Bearing in mind the asymptotic expansion of the Bessel function for large argument, Eq. (26) is

consistent with

$$S^{I}_{E,H} = -ka\left\{(-1)^{\ell_1} A J_{2\ell_1}(\xi) \pm (-1)^{\ell_2} B(\bar{\Phi}) J_{2\ell_2}(\xi) \mp i(-1)^{\ell_3} C(\bar{\Phi}) J_{2\ell_2+1}(\xi)\right\} \quad (47)$$

where

$$A = \frac{\frac{1}{n}\sin\frac{\pi}{n}}{1-\cos\frac{\pi}{n}} , \quad (48)$$

$$\left.\begin{matrix} B(\bar{\Phi}) \\ C(\bar{\Phi}) \end{matrix}\right\} = \frac{\sin\frac{\pi}{n}}{2n}\left[\frac{1}{\cos\frac{\pi}{n}-\cos\frac{3\pi-2\bar{\Phi}}{n}} \pm \frac{1}{\cos\frac{\pi}{n}-\cos\frac{3\pi+2\bar{\Phi}}{n}}\right] , \quad (49)$$

and

$$\xi = 2ka \sin\bar{\Phi} . \quad (50)$$

In Eq. (47), ℓ_1, ℓ_2 and ℓ_3 can have any integer values, and Eq. (26) follows from (47) on inserting the leading term in the asymptotic expansion of each Bessel function.

In the limiting case of a disk (n = 2), Eqs. (48) and (49) give

$$A = \frac{1}{2} , \quad B(\bar{\Phi}) = 0 , \quad C(\bar{\Phi}) = \frac{1}{2\sin\bar{\Phi}} ,$$

and the resulting expression for $S^{I}_{E,H}$ is consistent with the disk solution (see Knott et al, 1970) if and only if

$$\ell_1 = 1 , \quad \ell_3 = 0 .$$

Moreover, for axial incidence ($\bar{\Phi} = 0$) with $n \neq 2$, we have

$$B(0) = B_o , \quad C = 0 ,$$

and the result now agrees with Eq. (44) only if $\ell_2 = 0$. The caustically-corrected expression for $S^{I}_{E,H}$ is therefore

$$S^{I}_{E,H} = ka\left\{A\, J_2(\xi) \mp B(\Phi)\, J_o(\xi) \mp i\, C(\Phi)\, J_1(\xi)\right\}, \tag{51}$$

where A, $B(\Phi)$ and $C(\Phi)$ are given in Eqs. (48) and (49). It can be verified that this reduces to the disk result when $n = 2$.

The general form of (51) is identical to that arrived at by Ross (1969) using somewhat different reasoning, and his expressions for $B(\Phi)$ and $C(\Phi)$ differ from those given here only in being replaced by their first order approximations for small Φ. Because of the non-uniformity of the small Φ expansions according as $n \neq 2$ or $n = 2$, it is not possible to recover the disk solution from Ross' result, and it therefore appears desirable to retain the more complicated forms for $B(\Phi)$ and $C(\Phi)$ given in Eq. (49) even though our primary interest is in cones of small angle.

Turning now to the second-order terms, we observe that on the axial caustic S^{II}_{H} is given by (45), and since $G(0) = E(0)$, the caustically-corrected expression is

$$S^{II}_{H} = \sqrt{\frac{ka}{\pi}}\, e^{2ika - i\frac{\pi}{4}}\, G(\Phi)\, f_H(\Phi)\ , \tag{52}$$

where $f_H(\Phi)$ is a function having the properties

$$f_H(\Phi) = 1\ , \qquad \Phi = 0,$$

$$\sim \frac{2\, e^{i\frac{\pi}{4}}}{\sqrt{\pi\, ka}\, \sin\Phi}\ , \qquad \Phi \text{ bounded away from zero.} \tag{53}$$

This is precisely the matching problem encountered in disk scattering, and following the reasoning given by Knott et al (1970), we take

$$f_H(\Phi) = M\left(\frac{1}{2}\sqrt{ka}\,\sin\Phi\right) \quad , \tag{54}$$

where M(x) is related to the Fresnel integral F(x) by

$$M(x) = \frac{2}{\sqrt{\pi}}\, e^{-ix^2 - i\frac{\pi}{4}} F(x) = \frac{2}{\sqrt{\pi}}\, e^{-i\frac{\pi}{4}} \int_x^\infty e^{i(y^2-x^2)}\, dy \, . \tag{55}$$

Hence

$$S_H^{II} = \sqrt{\frac{ka}{\pi}}\, e^{2ika - i\frac{\pi}{4}} G(\Phi)\, M\left(\frac{1}{2}\sqrt{ka}\,\sin\Phi\right) . \tag{56}$$

The procedure for E polarization is very similar, and leads to the caustically-corrected expression

$$S_H^{II} = -\sqrt{\frac{ka}{\pi}(1+\sin^2\Phi)}\,\cos^2\Phi\, e^{2ika\sqrt{1+\sin^2\Phi} - i\frac{\pi}{4}} E(\Phi)\, M^*\left(\frac{1}{2}\sqrt{ka}\,\sin\Phi\right) , \tag{57}$$

where M(x) is as given in Eq. (55) and the asterisk denotes the complex conjugate.

4. Discussion and Experimental Comparison

The wide angle scattering formulae can be recovered from the caustically-corrected results of the previous section by replacing the Bessel functions (in the case of the first order contribution) and the Fresnel integral (second order contribution) by the leading terms in their asymptotic expansions for large argument. In this connection we note that $J_2(x)$ is approximated by its leading term within 10 percent only if $x \gtrsim 16$ (implying $\Phi \gtrsim 23^\circ$ for ka = 20), and F(x) is approximated by its leading term within 10° in phase (7 percent in amplitude) only if

$x > 1.42$ (implying $\Phi > 39^{\circ}$ for ka = 20). Thus, even for ka as large as 20 it is desirable to retain the more general expressions given in Eqs. (51), (56) and (57) over an extended range of Φ, and certainly throughout the entire backward cone if $\gamma \lesssim 20^{\circ}$.

The results derived so far are applicable for $0 < \Phi < \gamma$, where all the flash points P_1, P_2, P_3 and P_4 are illuminated. For $\gamma < \Phi \leq \Phi_{max.}$, P_2 is shadowed by the slant surface of the cone, and for $\Phi_{max} < \Phi$, P_3 and P_4 are also shadowed. In a purely asymptotic sense, a flash point can no longer contribute once it is shadowed. Consequently, for $\gamma < \Phi \leq \Phi_{max}$, S_H^{II} must be taken zero and $S_{E,H}^{I}$ replaced by the direct contribution attributable to P_1 alone (i.e. the terms involving $\exp(-2ika \sin \Phi)$ in Eq. (26)), thereby creating a discontinuity in S at $\Phi = \gamma$. Although this is the procedure that will be followed, in practice there is no such abrupt change in the contribution of a flash point on passing into the shadow since energy can still reach it by "creeping" over the curved surface of the cone.

In order to test the theory, a series of cw backscatter measurements was carried out using a cone with base radius 1.968 inches and half angle $\gamma = 15^{\circ}$ (for which $\Phi_{max} = 30.6^{\circ}$). The patterns were recorded for $-30^{\circ} \leq \Phi \leq 30^{\circ}$ as the frequency was increased in steps of 0.1 GHz from 8.0 to 11.0 GHz. The corresponding values of ka spanned the range $8.383 \leq ka \leq 11.527$ and both E and H polarizations were employed.

A comparison of the theoretical and experimental data for the backscattering cross section at axial incidence as a function of ka is shown in Figure 3. Whereas the first order theory (Eqs. (6), (23) and (44)) displays no resonance at all, the second order theory (Eqs. (6), (23), (44) and (45)) is qualitatively correct but exaggerates the resonance. It would therefore appear that for a precise estimate

of cone scattering, ka must be substantially greater than the values considered in Figure 3 or, alternatively, that the theory must be revised still further by the inclusion of third (and perhaps higher) order effects. Figure 3 also suggests the type of agreement to be expected at oblique angles: though we can look for the second order theory to reproduce the qualitative features of the angular behavior better than the first, the quantitative accuracy could be poorer if ka is in the range from 9.2 to 10.5. This is indeed what is found.

Results for ka = 9.641 are shown in Figures 4 and 5, with the measured patterns for H and E polarizations being given on the left and right respectively of each figure. The first order predictions are included in Figure 4, and throughout the entire backward cone the agreement is rather good, particularly for H polarization. For $\Phi > \gamma$, however, the first order estimate for E polarization is much too small, but this defect is remedied on including the second order term (see Figure 5) at the expense of a worsening of the agreement within the backward cone. A similar comparison for ka = 11.527 is given in Figures 6 and 7, and as anticipated from Figure 3, the second order theory is now better both qualitatively and quantitatively.

5. Conclusion

In this paper, two new results have been obtained: the second-order terms in the high-frequency expansions of the far-field coefficients for oblique backscattering from a flat-based cone have been derived, and a match has been provided between these wide-angle formulae and the known return for axial incidence. The resulting uniform expansions are valid for all cone angles, and are in good agreement with experiment at sufficiently high frequencies (ka greater than 11 or so).

A more accurate theoretical description of the backscattering would require the determination of terms higher than the second in the expansions of the far-field

coefficients. Specifically, creeping-wave phenomena and higher-order interactions between diffracting elements would have to be considered. While the former contribution could be determined without difficulty, the latter would entail laborious calculations because of the increased number of optical rays and because terms beyond the dominant one would have to be included in the expansions for the diffraction coefficients.

References

Bechtel, M.E. (1965), Application of geometric diffraction theory to scattering from cones and disks, Proc. IEEE 53, 877-882.

Bowman, J.J., T.B.A.Senior and P.L.E.Uslenghi (1969), Electromagnetic and acoustic scattering by simple shapes, North-Holland Publishing Co., Amsterdam.

Buchal, R.N. and J.B.Keller (1960), Boundary layer problems in diffraction theory, Commun. Pure Appl. Math. 13, 85-114.

Felsen, L.B. (1957), Plane-wave scattering by small-angle cones, IRE Trans. Antennas Propagat. 5, 121-129.

Keller, J.B., and E.B.Hansen (1965), Survey of the theory of diffraction of short waves by edges, Acta Phys. Polon. 27, 217-234.

Keller, J.B. (1960), Backscattering by a finite cone, IEEE Trans. Antennas Propagat. 8, 175-182.

Keller, J.B. (1961), Backscattering from a finite cone — comparison of theory and experiment, IRE Trans. Antennas Propagat. 9, 411-412.

Keller, J.B. (1957), Diffraction by an aperture, J. Appl. Phys. 28, 426-444.

Keller, J.B. (1962), Geometrical theory of diffraction, J. Opt. Soc. Amer. 52, 116-130.

Knott, E.F., T.B.A.Senior and P.L.E.Uslenghi (1970), High-frequency backscattering from a metallic disk, submitted to Proc. IEE (London).

Ross, R.A. (1969), Small-angle scattering by a finite cone, IEEE Trans. Antennas Propagat. 17, 241-242.

Ryan, C.E., Jr., and L. Peters, Jr. (1969), Evaluation of edge-diffracted fields including equivalent currents for the caustic regions, IEEE Trans. Antennas Propagat. 17, 292-299.

Ryan, C.E., Jr., and L. Peters, Jr. (1970), Correction to "Evaluation of edge-diffracted fields including equivalents for the caustic regions", IEEE Trans. Antennas Propagat. 18, 275.

Siegel, K.M. (1958), Far field scattering from bodies of revolution, Appl. Sci. Res. 7 (B), 293-328.

Ufimtsev, P. Ia. (1958), Secondary diffraction of electromagnetic waves by a disk, Soviet Phys.-Tech. Phys. 3, 549-556.

Appendix: Diffraction Matrix for a Wedge

To find the contribution to the field resulting from diffraction at the base of the cone, it is convenient to introduce the concept of a diffraction matrix appropriate to the local edge geometry, namely, to a wedge of half angle Ω, where $2\Omega = \frac{\pi}{2} - \gamma$.

To this end, consider a perfectly conducting wedge whose edge coincides with the z axis of a Cartesian coordinate system (x, y, z) and whose surfaces are defined by the equations $y = \pm x \tan \Omega$, $x \geq 0$, $-\infty < z < \infty$. The problem of a plane wave incident in a plane perpendicular to the z axis with either its electric or magnetic vector parallel to the edge is a classical one, the exact solution of which is known (see, for example, Bowman et al, 1969, pp 254 et seq.), and from these two basic results it is a trivial matter to deduce the corresponding solutions for plane waves incident at an angle $\pi - \beta$ to the z axis.

Instead of stating these solutions in terms of the original coordinates (x, y, z), we shall, following Keller (1957), define a new set of base vectors $\hat{T}, \hat{N}, \hat{B}$, where $\hat{T}$ is a unit vector parallel to the edge, $\hat{N}$ is a unit vector 'normal' to the edge and pointing away from the wedge, and $\hat{B}$ is the unit vector 'binormal' to the edge and pointing into the shadowed half space. The direction of $\hat{T}$ is chosen to make $\hat{T}, \hat{N}, \hat{B}$ a right-handed system, i.e. $\hat{T} = \hat{N} \times \hat{B}$. Specifically, and for maximum generality, we choose

$$\begin{aligned} \hat{T} &= -\hat{z} \ , \\ \hat{N} &= -\hat{x} \cos\delta + \hat{y} \sin\delta \ , \\ \hat{B} &= -\hat{x} \sin\delta - \hat{y} \cos\delta \ , \end{aligned} \tag{A.1}$$

where δ is arbitrary. Then if the incident electric field is

$$\underline{E}^i = \hat{e}^i e^{ik \hat{i} \cdot \underline{r}} \tag{A.2}$$

with

$$\hat{i} = \hat{T} \cos\beta - \hat{N} \sin\beta \sin\alpha + \hat{B} \sin\beta \cos\alpha \ , \tag{A.3}$$

$$-\frac{\pi}{2} + \Omega + \delta \leq \alpha \leq \frac{\pi}{2} + \delta, \qquad 0 < \beta < \pi \ ,$$

the diffracted electric field at points far from the edge and away from all geometrical optics boundaries can be written as

$$\underline{E}^d = \hat{e}^d \left(-\frac{e^{i\frac{\pi}{4}}}{\sin\beta \sqrt{2\pi ks}} \right) e^{ik \hat{s} \cdot \underline{r}} \tag{A.4}$$

with

$$\hat{s} = \hat{T} \cos\beta + \hat{N} \sin\beta \sin\theta - \hat{B} \sin\beta \cos\theta \ , \tag{A.5}$$

$$-\frac{\pi}{2} + \Omega + \delta \leq \theta \leq \frac{3\pi}{2} - \Omega + \delta, \qquad 0 < \beta < \pi \ \blacktriangle \ . \tag{A.6}$$

In particular, if

$$\hat{e}^i = \hat{T} \sin\beta + \hat{N} \cos\beta \sin\alpha - \hat{B} \cos\beta \cos\alpha \ , \tag{A.7}$$

then

$$\hat{e}^d = -(\hat{T} \sin\beta - \hat{N} \cos\beta \sin\theta + \hat{B} \cos\beta \cos\theta)(X - Y) \ ,$$

and if

$$\hat{e}^i = \hat{N} \cos\alpha + \hat{B} \sin\alpha \ , \tag{A.8}$$

then

$$\hat{e}^d = (\hat{N} \cos\theta + \hat{B} \sin\theta)(X + Y) \ ,$$

where

$$X = \frac{1}{n} \sin\frac{\pi}{n} \left\{ \cos\frac{\pi}{n} - \cos\frac{1}{n}(\alpha - \theta) \right\}^{-1}$$

$$Y = \frac{1}{n} \sin\frac{\pi}{n} \left\{ \cos\frac{\pi}{n} + \cos\frac{1}{n}(\pi + 2\delta - \alpha - \theta) \right\}^{-1} \qquad (A.9)$$

with

$$n = 2\left(1 - \frac{\Omega}{\pi}\right) = \frac{3}{2} + \frac{\gamma}{\pi} \quad . \qquad (A.10)$$

These are the asymptotic forms of the two fundamental solutions referred to earlier, and it will be noted that

$$\hat{i} \cdot \hat{e}^i = 0 = \hat{s} \cdot \hat{e}^d \quad .$$

We can cast the above results in the form of a diffraction matrix by writing

$$\hat{e}^d = \Delta \hat{e}^i \qquad (A.11)$$

where $\hat{e}^i$ is now treated as a column vector in the base $\hat{T}$, $\hat{N}$, $\hat{B}$ and Δ is a 3 x 3 matrix (or dyadic). Although a general diffraction matrix is unique, Eqs. (A.7) and (A.8) yield only 6 equations for the determination of the 9 matrix elements. The resulting arbitrariness is a consequence of considering only incident plane waves, and an observation point characterised by the same angle β as the incident field at large distances from the edge where the diffracted field is also locally plane. If the matrix elements deduced from Eqs. (A.7) and (A.8) are expressed in terms of the elements in the final column, and the latter are then put equal to zero, we obtain the following matrix:

$$\Delta = \begin{pmatrix} -(X-Y) & 0 & 0 \\ -\left\{X\sin(\alpha-\theta)+Y\sin(\alpha+\theta)\right\}\dfrac{\cot\beta}{\cos\alpha} & (X+Y)\dfrac{\cos\theta}{\cos\alpha} & 0 \\ -\left\{X\cos(\alpha-\theta)-Y\cos(\alpha+\theta)\right\}\dfrac{\cot\beta}{\cos\alpha} & (X+Y)\dfrac{\sin\theta}{\cos\alpha} & 0 \end{pmatrix} \tag{A.12}$$

This reduces to the diffraction matrix for a half plane on putting $\Omega = 0$ ($n = 2$) and, when $\delta = 0$, is equivalent to the half plane result given by Keller (1957) provided the elements in the second column of this matrix are reversed in sign (see Knott et al, 1970).

The above matrix is sufficient and entirely adequate if $\cos\alpha \neq 0$, but if $\alpha = \pm\pi/2$, a casual inspection of Eqs. (A.7) and (A.8) shows that the matrix is no longer correct. This failure is evidenced by three of the matrix elements becoming infinite, and since a knowledge of the result for $\alpha = -\pi/2$ is required for the determination of the second order diffraction term, this particular case cannot be ignored. Knott et al (1970) overcame the difficulty in their treatment of disk scattering by considering a slightly curved disk and, having found the second order term, by taking the limit as the disk became plane. The subterfuge is not necessary, however, and can be avoided by a simple modification of the matrix.

A form which is alternative to (A.12) and consistent with Eqs. (A.7) and (A.8) for all α is:

$$\Delta = \begin{pmatrix} -(X-Y) & 0 & 0 \\ (X-Y)\cot\beta\sin\theta & (X+Y)\cos\theta\cos\alpha & (X+Y)\cos\theta\sin\alpha \\ -(X-Y)\cot\beta\cos\theta & (X+Y)\sin\theta\cos\alpha & (X+Y)\sin\theta\sin\alpha \end{pmatrix} \tag{A.13}$$

It is trivial to show that the difference between (A.13) and (A.12) implies a null field for all incident plane waves having $\cos\alpha \neq 0$, but in contrast to (A.12), (A.13) is in accordance with (A.7) and (A.8) when $\cos\alpha = 0$. The elements of (A.13) are, moreover, simpler than those of (A.12), and though (A.13) has additional non-zero elements, its universality more than compensates for this inconvenience.

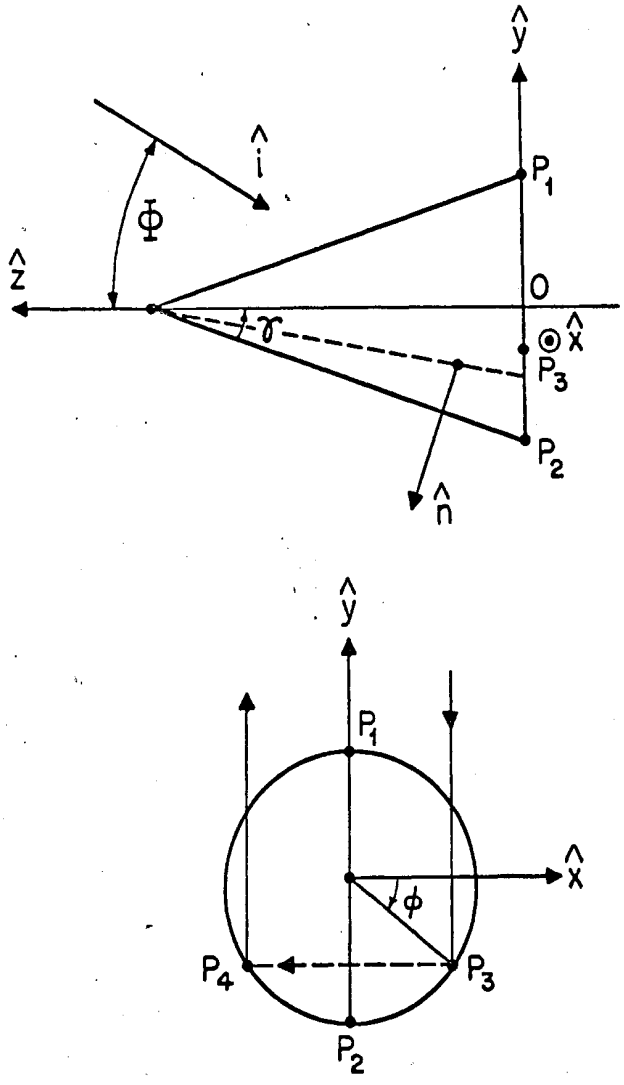

Figure 1: Geometry of the scattering problem viewed from (a) the side and (b) the tip of the cone.

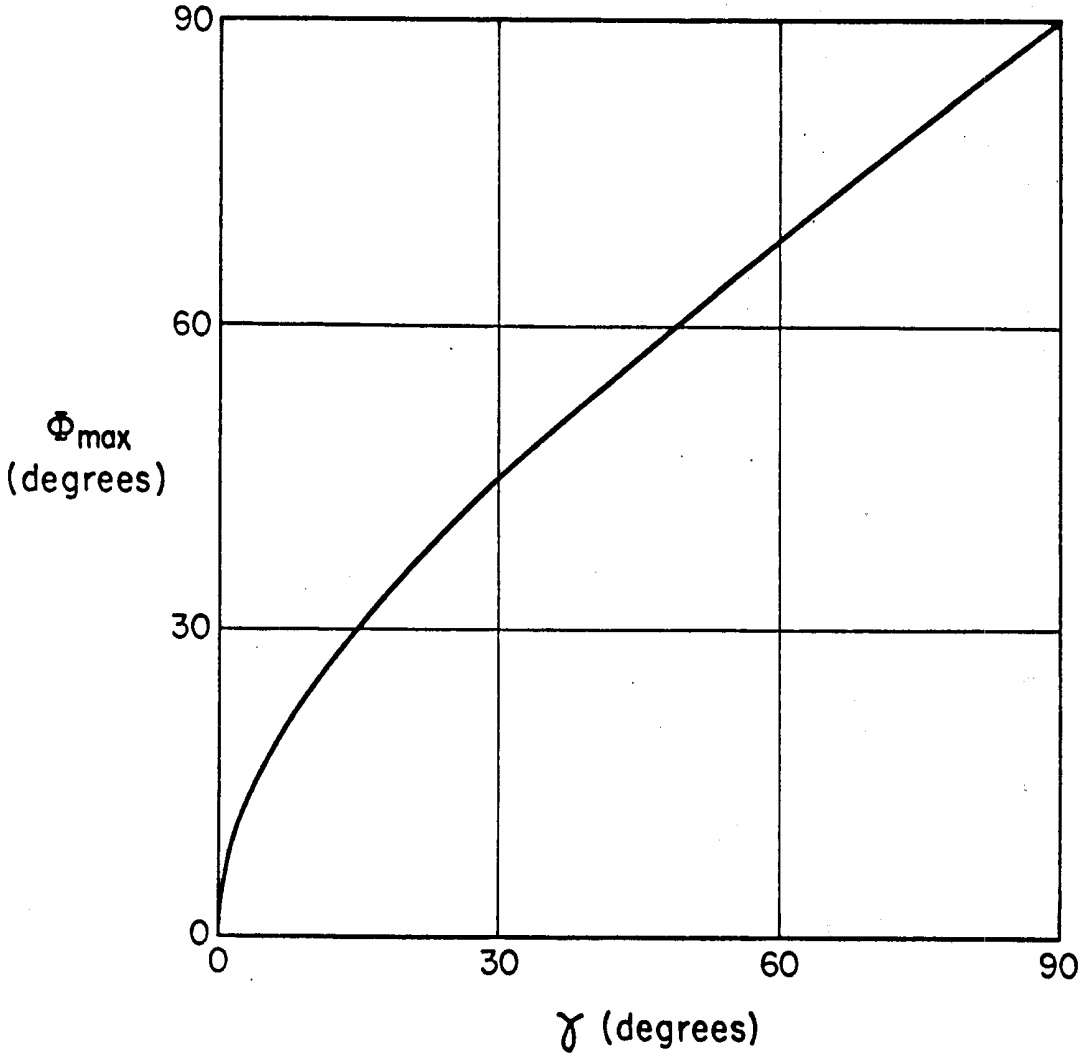

Figure 2: The behavior of Φ_{max} as a function of γ.

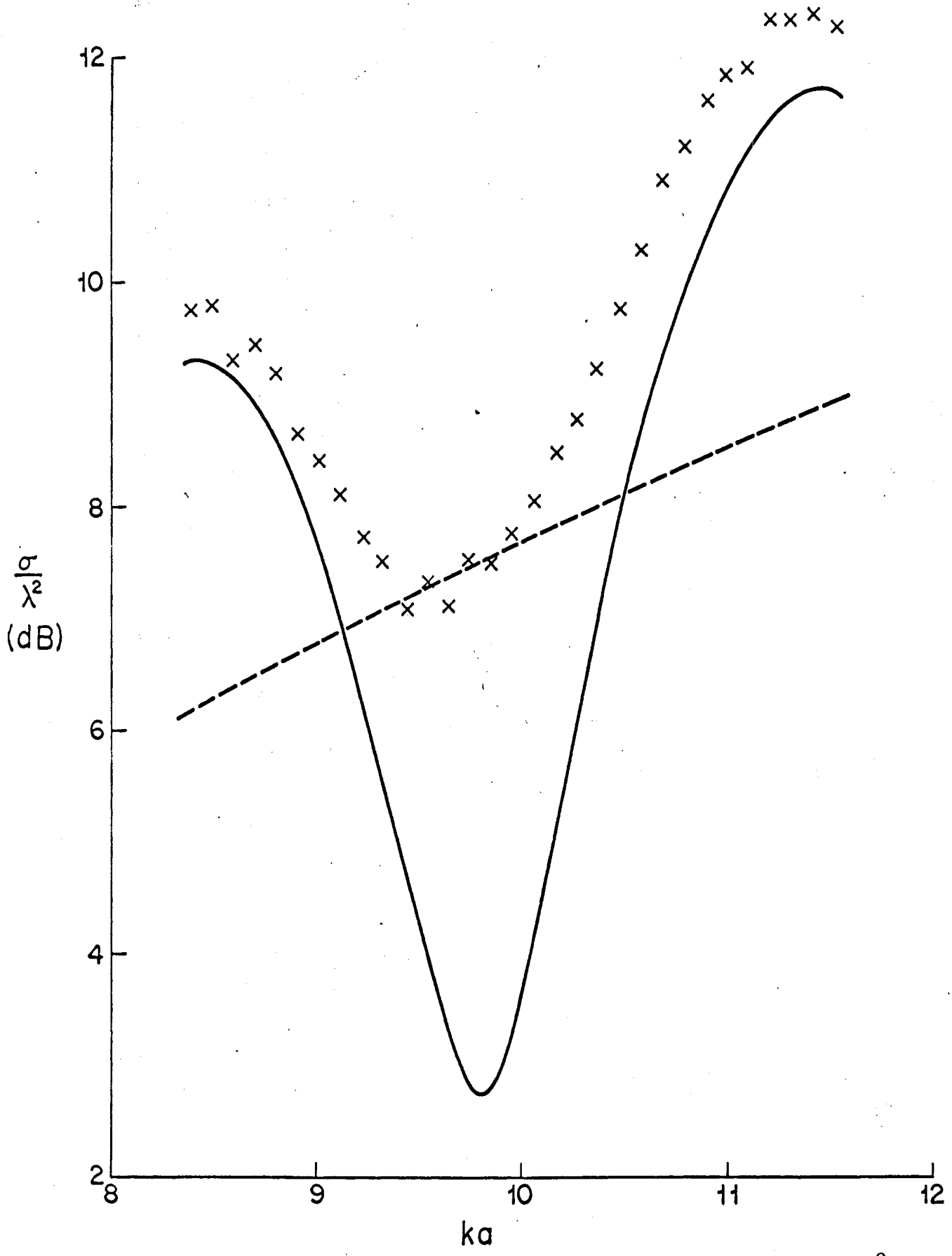

Figure 3: Comparison of theory and experiment for axial incidence with $\gamma = 15^{o}$: (x x x) experiment, (- - -) first order theory, (——) second order theory.

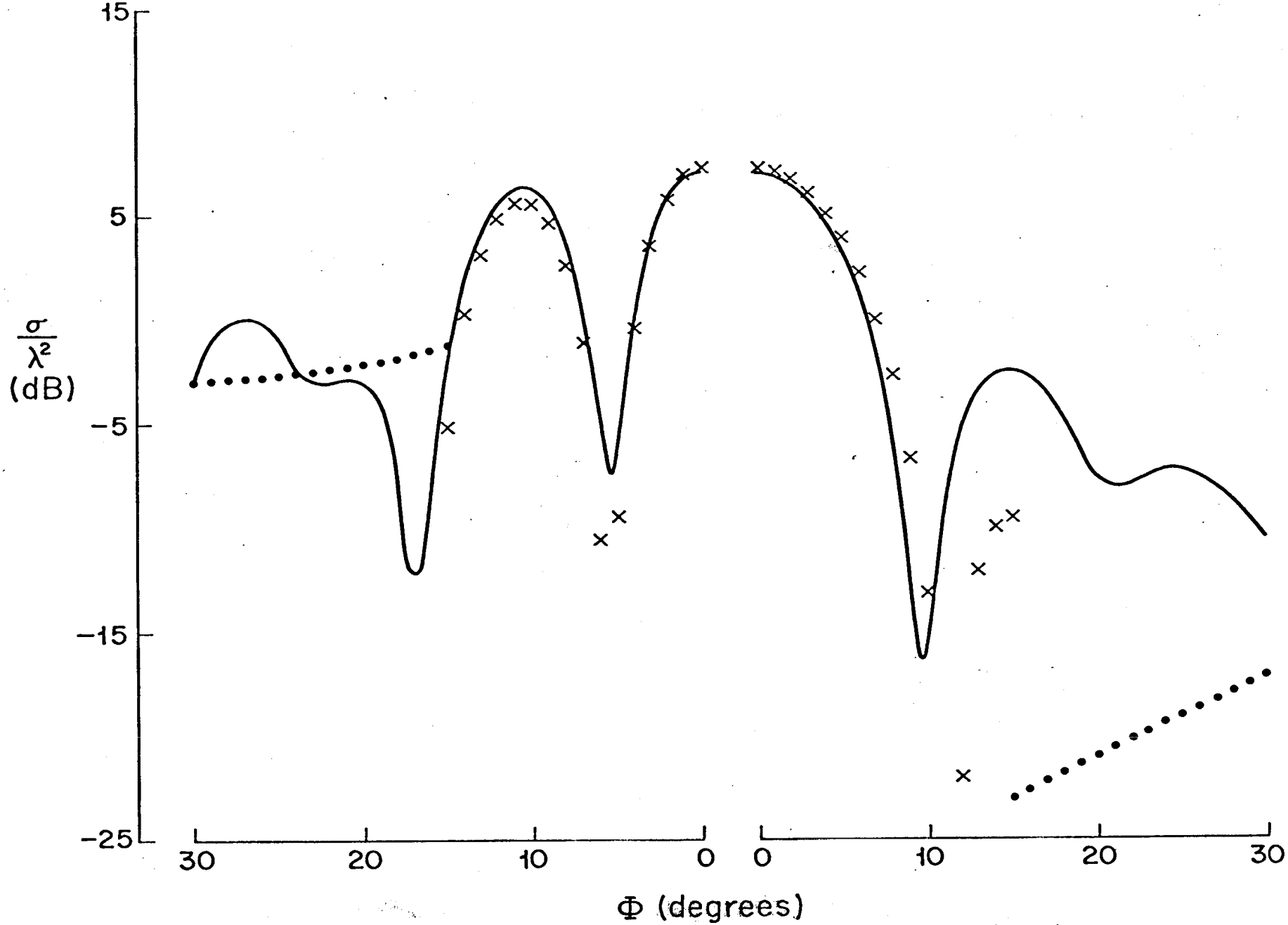

Figure 4: Comparison of the first order theory, (x x x, • • •) with experiment (——) for ka = 9.661 and α = 150. H-polarization on the left and E-polarization on the right.

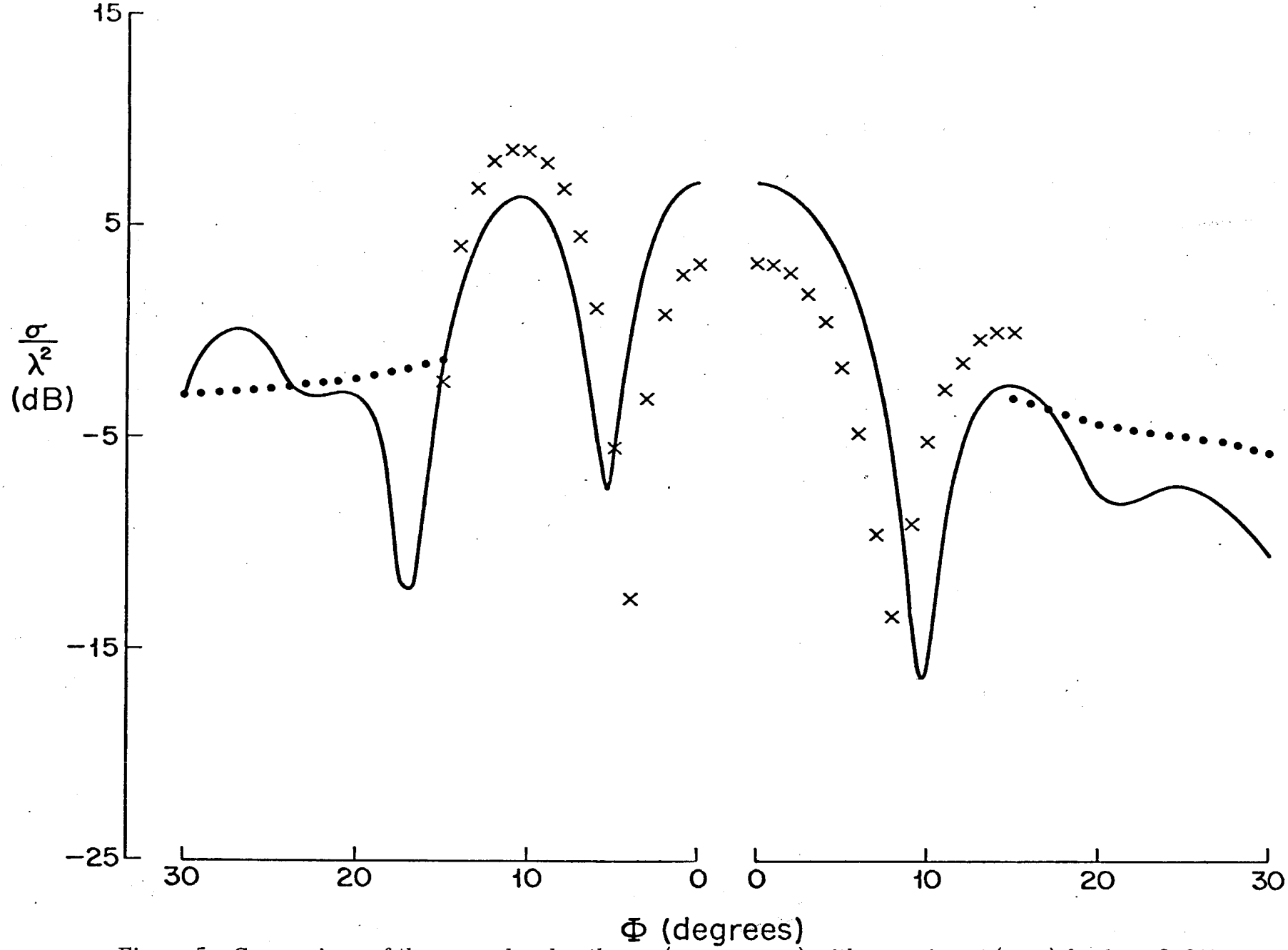

Figure 5: Comparison of the second order theory (x x x, • • •) with experiment (——) for ka = 9.641 and $\gamma = 15^{o}$. H-polarization on the left and E-polarization on the right.

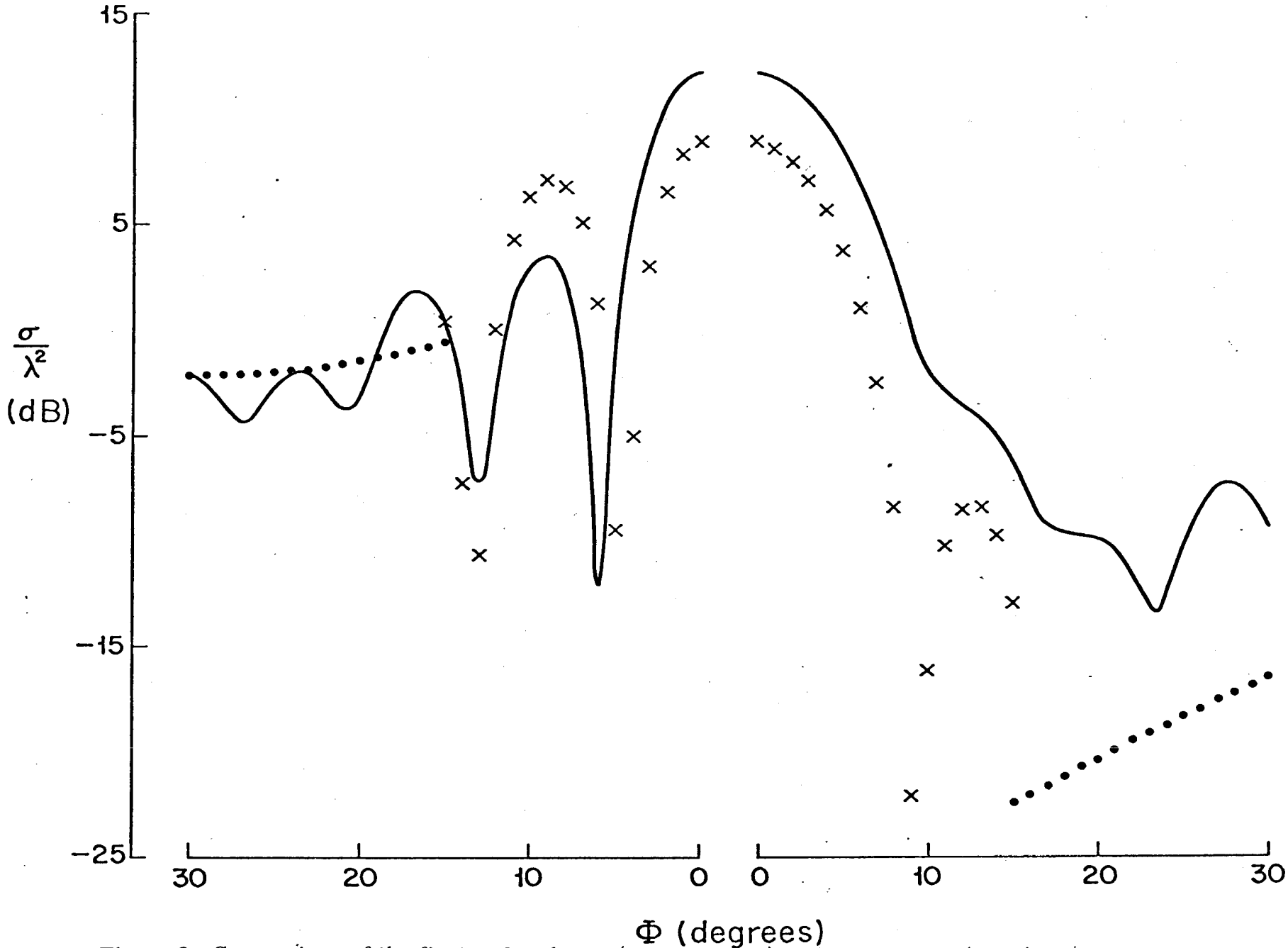

Figure 6: Comparison of the first order theory (x x x , • • •) with experiment (——) for ka = 11.527 and $\alpha = 15^{o}$. H-polarization on the left and E-polarization on the right.

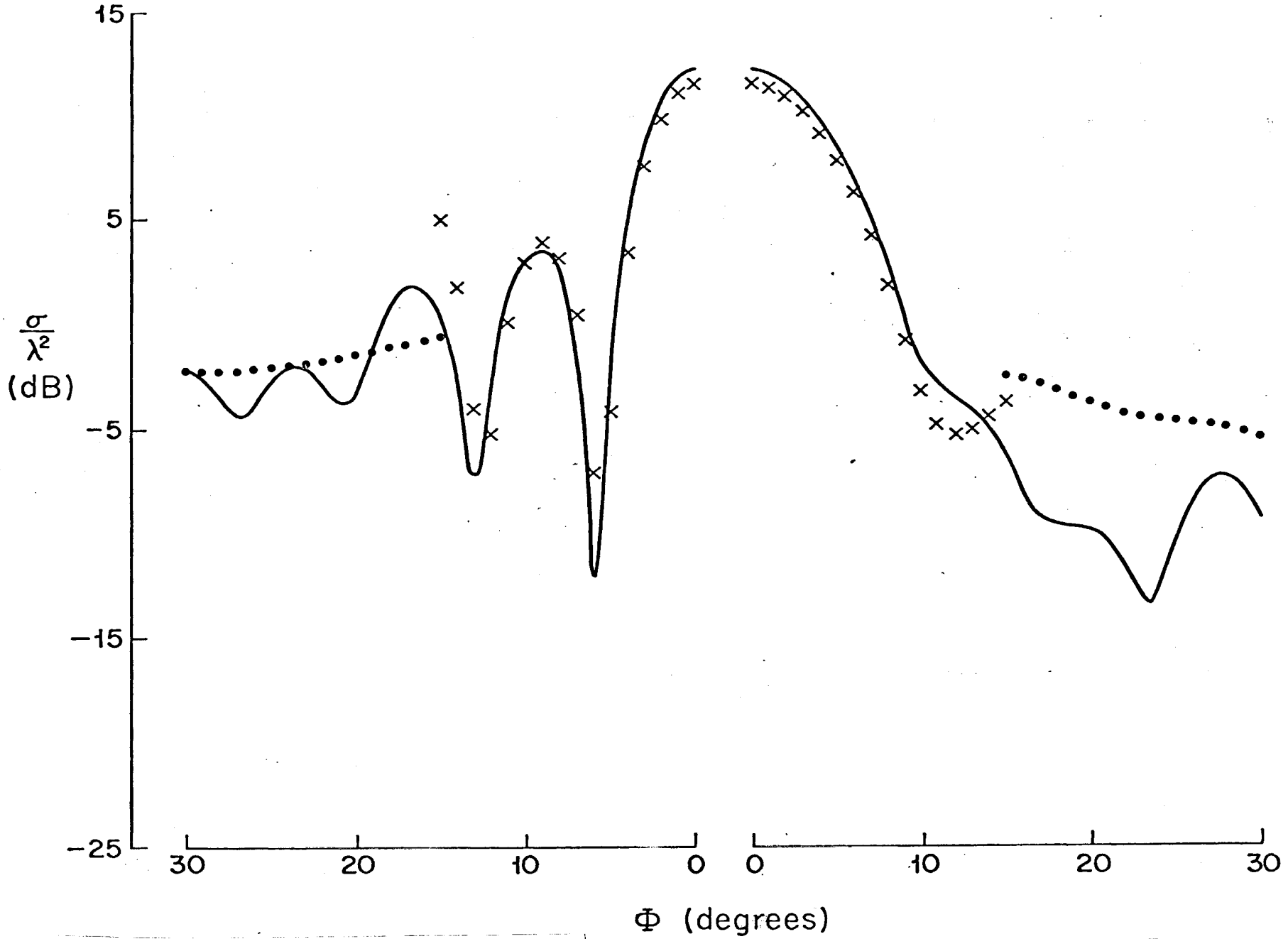

Figure 7: Comparison of the second order theory (x x x, • • •) with experiment (——) for ka = 11.527

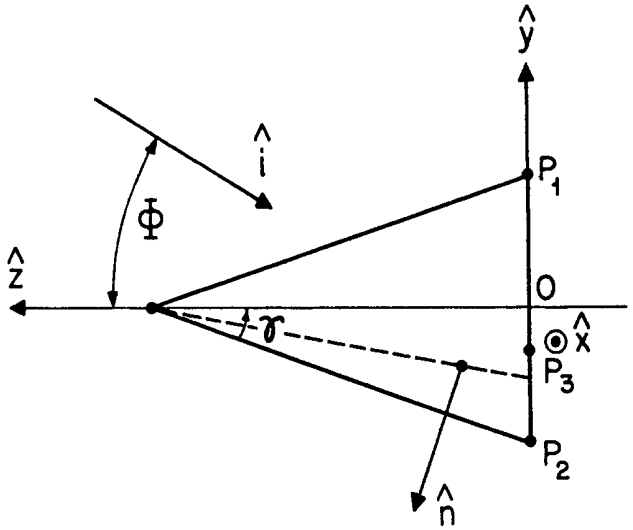
ŷ
î
Φ
P1
ẑ
0
γ
x̂
P3
P2
n̂

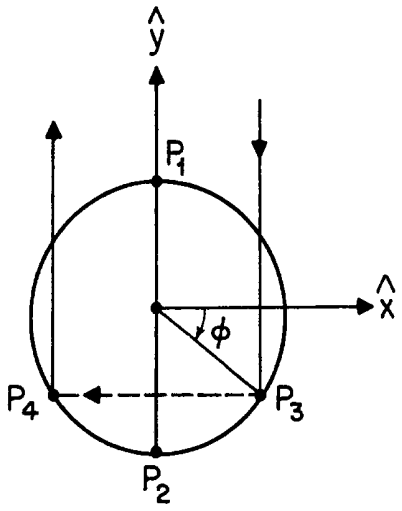
ŷ
P1
x̂
φ
P4
P3
P2

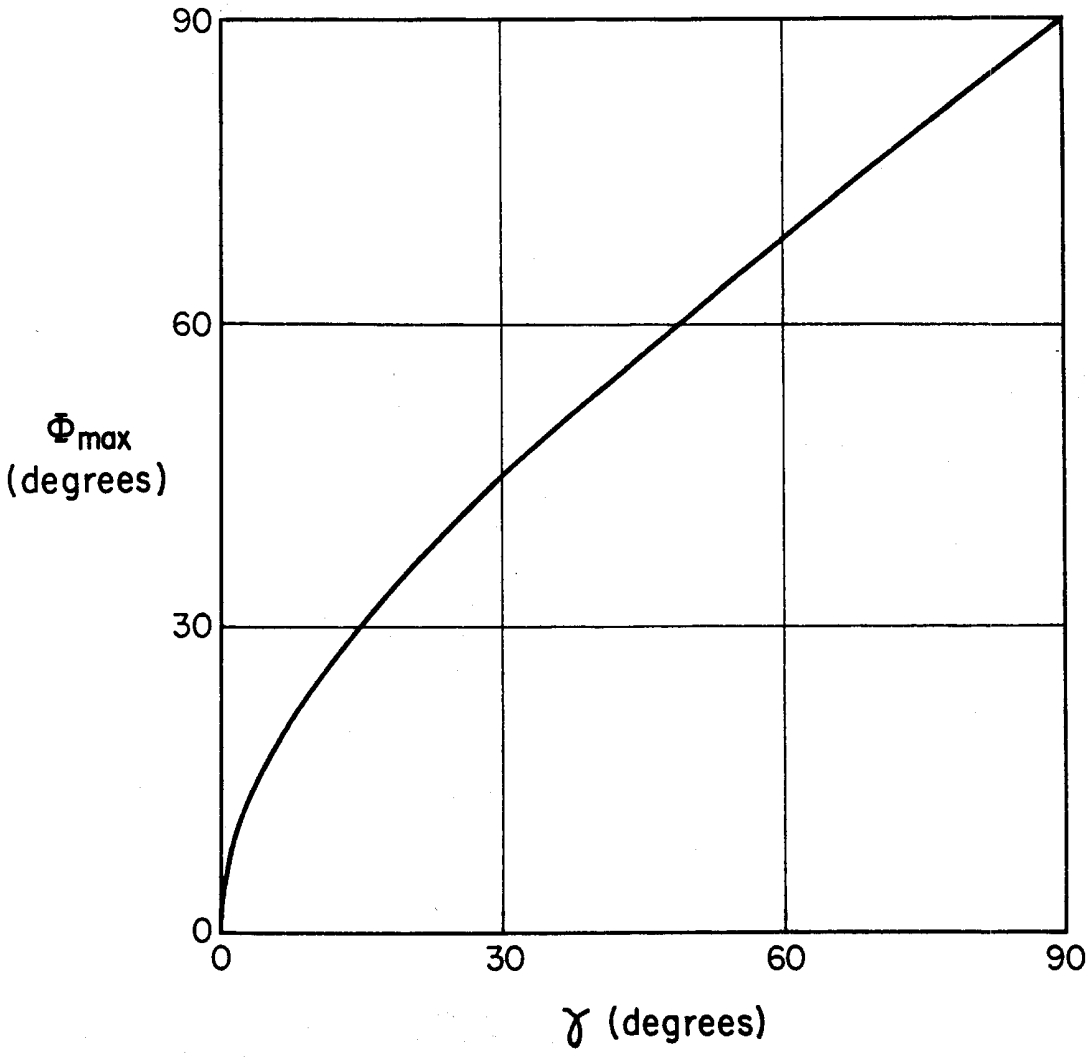
90
60
30
0
Φ_{max}
(degrees)
0
30
60
90
γ (degrees)